Toll-Like Receptor-4 Modulates Survival by Induction of Left Ventricular Remodeling after Myocardial Infarction in Mice[1]

Alexander Riad,* Sebastian Jäger,* Meike Sobirey,* Felicitas Escher,* Aymaru Yaulema-Riss,* Dirk Westermann,* Aysun Karatas,‡ Markus M. Heimesaat,† Stefan Bereswill,† Duska Dragun,‡ Matthias Pauschinger,* Heinz P. Schultheiss,* and Carsten Tschöpe[2]*

Left ventricular (LV) remodeling is known to contribute to morbidity and mortality after myocardial infarction (MI). Because LV remodeling is strongly associated with an inflammatory response, we investigated whether or not TLR-4 influences LV remodeling and survival in a mice model of MI. Six days after MI induction, TLR4 knockout (KO)-MI mice showed improved LV function 32 and reduced LV remodeling as indexed by reduced levels of atrial natriuretic factor and total collagen as well as by a reduced heart weight to body weight ratio when compared with WT-MI mice. This was associated with a reduction of protein levels of the intracellular TLR4 adapter protein MyD88 and enhanced protein expression of the anti-hypertrophic JNK in KO-MI mice when compared with wild-type (WT)-MI mice. In contrast, protein activation of the pro-hypertrophic kinases protein kinase Cδ and p42/44 were not regulated in KO-MI mice when compared with WT-MI mice. Improved LV function, reduced cardiac remodeling, and suppressed intracellular TLR4 signaling in KO-MI mice were associated with significantly improved survival compared with WT-MI mice (62 vs 23%; $p < 0.0001$). TLR4 deficiency led to improved survival after MI mediated by attenuated left ventricular remodeling. ***The Journal of Immunology,*** **2008, 180: 6954–6961.**

Myocardial infarction (MI)[3] is a major cause of death in Western countries (1). One of the most important prognostic factors is the development of left ventricular (LV) remodeling. This includes a combination of concentric and excentric hypertrophy, cardiac fibrosis, and subsequent LV dysfunction leading to heart failure (2). Although the current treatment strategy affecting neurohumoral activation and thrombocyte aggregation has improved the outcome of patients markedly over the last decade, the cardiovascular risk after MI is still 10-fold elevated when compared with healthy humans (1). A new concept of initiating LV remodeling after MI revealed, from a solid body of evidence, that this disease is strongly associated with intense autoimmune inflammatory response to, among other things, cytokine release and cardiac infiltration of immune cells (3).

TLRs have been identified as key recognition components of the innate immune system in mammals and are known to be also involved in cardiac inflammatory response in heart failure (4–6). Evidence for a relevance of TLRs, especially TLR2 and TLR4, in the development of LV dysfunction has been derived mostly from experimental studies using different models of heart failure. In those studies, it had been shown that the absence of TLR2 led to improved LV function in animal models of MI, ischemia/reperfusion, and doxorubicin-induced cardiomyopathy (7–9). TLR4 is also of special interest because its activation results as well from endogenous and exogenous ligands such as fibrinogen, oxidized low density lipoprotein (LDL), and heat shock proteins known to be involved in heart failure or coronary heart disease (10–12). Stimulation of TLR4 can lead to a MyD88-dependent activation of several intracellular mediators such as kinases, including those also known to belong to key regulators of LV remodeling (13, 14). In addition, activation of the TLR4 pathway has recently been shown to directly impair the contractility of isolated myocytes (15). Furthermore, several experimental studies in models of LV hypertrophy, ischemia/reperfusion injury, and sepsis provide further evidence for a relevance of this receptor in the development of cardiovascular diseases.(9, 16–18) Studies in humans showed a correlation between TLR4 expression and myocardial ischemia, suggesting that this receptor might also play a clinical role (19, 20).

In the present study, we investigated whether or not TLR4 has an influence on cardiac remodeling, LV function, and survival in a mouse model of MI.

Materials and Methods

Animals

C57BL/10ScSn wild-type (WT) and TLR4-deficient (knockout or KO) mice (C57BL/10ScN, carrying a deletion of the TLR4 gene) were obtained from the breeding stocks of the Max-Planck-Institut für Immunologie (Freiburg, Germany) (21). All mouse strains were bred in the Forschungsinstitut für Experimentelle Medizin (Berlin, Germany). The investigation conforms to the guidelines set by the National Institutes of Health (Bethesda, MD) for the care and use of laboratory animals.

*Department of Cardiology and Pneumology and †Department of Microbiology, Campus Benjamin Franklin and ‡Department of Nephrology and Intensive Care Medicine, Campus Virchow Clinic and Center for Cardiovascular Research, Charité University Medicine, Berlin, Germany

Received for publication September 25, 2007. Accepted for publication March 1, 2008.

The costs of publication of this article were defrayed in part by the payment of page charges. This article must therefore be hereby marked *advertisement* in accordance with 18 U.S.C. Section 1734 solely to indicate this fact.

[1] This work was supported by a grant from the Deutsche Forschungsgesellschaft (TR-SFB 19, project Z3 and B2) to C.T.

[2] Address correspondence and reprint requests to Dr. Carsten Tschöpe, Department of Cardiology and Pneumology, Charité-University Medicine Berlin, Campus Benjamin Franklin, Hindenburgdamm 30, 12200 Berlin, Germany. E-mail address: carsten.tschoepe@charite.de

[3] Abbreviations used in this paper: MI, myocardial infarction; ANF, atrial natriuretic factor; dP/dt_{max}, maximal rate of LV pressure rise (mm HG/s); dP/dt_{min}, minimal rate of LV pressure fall (mm HG/s); KO, knockout (TLR4-deficient mice); LV, left ventricular; LVEDP, LV end diastolic pressure; LVP, LV peak systolic pressure; p (prefix), phosphorylated; PKCδ, protein kinase Cδ; WT, wild type.

Surgical procedure

MI was induced in WT (WT-MI) and KO (KO-MI) mice by permanent ligation of the left descending coronary artery as described previously (22, 23). Sham-operated mice (WT and KO) underwent the same surgical procedure without ligation of the coronary artery and served as controls. Only animals with similar infarct sizes (>50%), which were evaluated macroscopically, were included in the study. For a mortality study, WT-MI and KO-MI mice ($n = 60$ per group) were kept for 4 wk. In a second set, WT, KO, WT-MI, and KO-MI mice were anesthetized (thiopental i.p. at 125 μg/g), intubated, and artificially ventilated ($n = 8$ per group) 6 days after MI induction. For this set, WT-MI and KO-MI mice ($n = 15$ per group) were operated on, and for animals with similar MI sizes >50% were included in our study ($n = 8$ per group). Sham-operated WT and KO mice served as controls ($n = 8$ per group). LV peak systolic pressure (LVP; in mm Hg), the maximal rate (max) of LV pressure rise ($dP/dt_{max.}$; in mmHg/s), heart rate (in beats per minute), LV end diastolic pressure (LVEDP; in mmHg), and the minimal rate (min) of LV pressure fall ($dP/dt_{min.}$; in mm Hg/s) as indices of LV systolic and diastolic function were recorded via a Millar Mikro-tip catheter (1.4 French) system in closed chest animals as described previously (24).

Myocardial infarction size

After hemodynamic measurements, MI size was determined macroscopically in a blinded session and semiquantitatively separated into two groups, namely small (+) and large (++) MI size. This method was chosen to save LV tissue for molecular biological and immunohistological analyses. To validate this method, in a pilot study we performed MI induction in WT mice ($n = 10$). In a blinded session we determined MI size as described above. After that, whole hearts were embedded in paraffin and 30 3-μm-thick LV transverse sections per heart were stained with hemalaun-eosin. The MI area was quantified by digital image analysis as described previously (25). MI size of eight animals was macroscopically scaled as large (++). This corresponded to a MI size of 55 ± 4% as determined by digital image analysis. The low SD of histologically calculated MI size clearly demonstrates the validity of macroscopic determination of MI size.

Tissue preparation

After hemodynamic measurements, LV tissues that had been separated into infarcted and noninfarcted areas were then snap frozen immediately in liquid nitrogen and stored at −80°C for molecular biological analyses. Further, serial 3-μm-thick, transverse, 4% buffered formalin-fixed LV sections were embedded in paraffin for histological analyses.

Immunostaining of CD3-positive T-lymphocytes and Sirius Red staining of total collagen content

Total cardiac collagen content of the Sirius Red (Polysciences)-stained sections was measured in the noninfarcted LV under circularly polarized light and quantified by digital image analysis as described elsewhere ($n = 6$ per group) (26). As described previously, immunostaining of CD3-positive T cells in the infarcted and noninfarcted areas was conducted with goat anti-CD3 (1:25; Santa Cruz Biotechnology) The EnVision peroxidase-conjugated rabbit-anti-goat Ab (DakoCytomation) was used as the secondary Ab according to the manufacturer's instructions (27). The ratio between heart tissue area and chromogen Sirius Red positive area was calculated (depicted here as area fraction (%)). The amount of CD3-positive cells was calculated by cells per area of heart tissue (cells/mm^2).

TUNEL assay in the infarcted area

In paraffin tissue sections we detected apoptotic cells by end labeling the fragmented DNA using the DeadEnd Colorimetric TUNEL system (Promega) according to the manufacturer's instructions. The slides were examined in a blinded fashion. TUNEL-positive cells were calculated as cells per area of heart tissue at 200-fold magnification.

Quantitative real-time RT-PCR (TaqMan) of atrial natriuretic factor (ANF) in the noninfarcted area

For RNA preparation, LV tissue samples of the noninfarcted area ($n = 6$ per group) were homogenized and total RNA was prepared using the TRIzol reagent (Invitrogen) according to the manufacturer's protocol. Quantitative real-time RT-PCR was performed on an ABI PRISM 7700 sequence detection system using the TaqMan universal master mix (Applied Biosystems). TaqMan gene expression was used to quantify the ANF mRNA expression (assay identifier: Mm01255747 g1; Applied Biosystems). All samples were run in triplicate. Relative gene expression as well as the fold amount difference between samples was calculated using the ΔΔCt threshold cycle method (28).

LightCycler-based RT-PCR assay

The LightCycler PCR and detection system (Roche) was used for amplification and online quantification. For this study we used oligo(dT) primers (TIB MOLBIOL) specific for conserved regions of mice TGF-β1, The following primer pair was used: 5′-CTAATGGTGGACCGCAACAAC-3′ (sense) and 5′-CGGTTCATGTCATGGATGGTG-3′ (antisense) for TGF-β1. The PCR mixture contained H_2O, *Taq* polymerase, 3 mM magnesium chloride, Master SYBR Green mix (Roche), and specific primers. The cycle numbers of the logarithmic linear phase were plotted against the logarithm of the concentration of template DNA. The concentrations of DNA in the samples were calculated by comparing the cycle numbers of the logarithmic linear phase of the samples with the cycle numbers of the external standards. All samples were analyzed in two or three parallel groups. Results of amplification of the standards and samples were verified on a 1% agarose gel. No unspecific amplification product was documented.

Western blot analysis in the noninfarcted area

Western blot analyses ($n = 6$ per group) were performed using primary Abs raised against total AKT (1/1000; Cell Signaling), phosphorylated AKT (pAKT) (1/1000; Cell Signaling), total protein kinase Cδ (PKCδ) (1/1000; Cell Signaling), phosphorylated PKCδ (pPKCδ) (1/1000; Cell Signaling), total p42/44 (1/1000; Cell Signaling), phosphorylated p42/44 (pp42/44) (1/1000; Cell Signaling), total JNK (1/1000; Cell Signaling), phosphorylated JNK (pJNK) (1/1000; Cell Signaling), calcineurin (1/250; BD Biosciences), and MyD88 (1/1000; Imgenex) that were incubated with 5% milk overnight or for 1 h at room temperature, respectively. Chemiluminescence detection was performed with ECL Plus (Amersham Pharmacia Biotech) and chemiluminescence was also detected by the use of x-ray films. MyD88 expression was normalized to GAPDH (1/2000; BD Biosciences). Other proteins were normalized by their inactive, nonphosphorylated forms. Quantitative measurement was performed using TINA software.

Statistical analysis

Statistical analysis was performed using SPSS version 12.0. Data are expressed as the mean ± SEM. Statistical differences were assessed by using the Kruskal-Wallis test in conjunction with the Mann-Whitney *U* posthoc test. Survival curves after MI were created by using the Kaplan-Meier method and compared by using the log-rank test. Statistical significance was accepted at a value of $p < 0.05$.

Results

LV function

To determine the degree of heart failure 6 days after induction of MI, we measured LV function in vivo as well as dry and wet lung weight to quantify pulmonary edema (Table I). No parameter of systolic and diastolic LV function was seen to differ between sham-operated WT and KO mice. WT-MI mice displayed impaired systolic and diastolic (LVP, −28%; dP/dt_{max}, −51%; LVEDP, +450%; dP/dt_{min}, −44%; heart rate, −24%; $p < 0.05$) LV function associated with increased wet lung weight as an index of pulmonary edema (+33%, $p < 0.05$) and heart failure. In contrast, among KO-MI mice LV function was significantly improved (LVP, +17%; dP/dt_{max}, +59%, LVEDP, −36%; dP/dt_{min}, +37%; $p < 0.05$) in comparison with that of WT-MI mice. This was associated with a decrease in wet lung weight (−22%; $p < 0.05$) (Table I).

LV remodeling of the noninfarcted area

Along with hemodynamic changes, we determined the markers of LV remodeling 6 days after the induction of MI in the noninfarcted area. In WT-MI mice the heart weight (+25%), heart weight to body weight ratio (45%), and total collagen content (+80%) as well as the mRNA contents of ANF (+210%) and TGF-β (+93%) were all significantly increased ($p < 0.05$) when compared with those of sham-operated WT mice (Fig. 1). These parameters of LV

Table I. *LV function and lung weight*

	WT (n = 8)	KO (n = 8)	WT-MI (n = 8)	KO-MI (n = 8)
Heart rate (bpm)	364 ± 24	375 ± 65	276 ± 33*	282 ± 59*
LV pressure (mm Hg)	96 ± 6	94 ± 7	69 ± 9*	81 ± 6#
dP/dt max (mm Hg/s)[a]	6228 ± 901	6256 ± 954	3042 ± 611*	4851 ± 823#
LV end diastolic pressure (mm Hg)	4 ± 1	5 ± 1	22 ± 2*	14 ± 3#
dP/dt min (mm Hg/s)[b]	−5127 ± 567	−5084 ± 615	−2894 ± 511*	3962 ± 647#
Lung weight dry (mg)	33 ± 4	31 ± 5	32 ± 4	34 ± 6
Lung weight wet (mg)	149 ± 19	147 ± 17	198 ± 43*	154 ± 26#

[a] Maximal rate of LV pressure rise.
[b] Minimal rate of LV pressure fall.
*, $p < 0.05$ vs WT; #, $p < 0.05$ vs WT-MI (n = 8 per group).
Data from in vivo assessment of LV function are expressed as mean ± SEM.

remodeling were significantly reduced in KO-MI mice when compared with WT-MI mice (heart weight, −11%; heart weight/body weight, −16%; total collagen, −45%; ANF, −44%; TGF-β, −43%; $p < 0.05$) (Fig. 1).

MyD88 protein expression after myocardial infarction in the noninfarcted area

MyD88 protein content in the noninfarcted area was up-regulated in WT-MI mice when compared with WT mice (+80%; $p < 0.05$) (Fig. 2). KO-MI mice displayed a reduction of MyD88 expression by 35% ($p < 0.05$). Moreover, in KO-MI mice no significant regulation was seen when compared with KO mice.

Cardiac protein activation of PKCδ, p42/44, JNK, and calcineurin

The existing body of work on this topic suggests that, among others, PKCδ, p42/44, JNK, and calcineurin are key mediators in the development of LV remodeling (14). Interestingly, such intracellular mediators have been shown to be involved in TLR signaling and regulation (29, 30). To investigate whether or not these mediators are modulated by TLR4 after MI, we measured its cardiac protein activation.

PKCδ and p42/44 protein activation after myocardial infarction in the noninfarcted area

In the noninfarcted area, the pPKCδ:PKCδ ratio and the pp42/44:p42/44 ratio were significantly up-regulated in WT-MI mice 6 days after MI induction in comparison to those of sham-operated WT mice (pPKCδ:PKCδ, +114%; pp42/44:p42/44, +257%; $p < 0.05$) (Fig. 3), indicating enhanced activity of these two kinases due to MI. Both the pPKCδ:PKCδ ratio and the pp42/44:p42/44 ratio were also up-regulated in KO-MI mice when compared with sham-operated KO mice (pPKCδ/PKCδ, +99%; pp42/44:p42/44, +183%; $p < 0.05$). In addition, there was no significant difference seen between WT-MI and KO-MI regarding these ratios.

Protein activation of JNK and the ratio of JNK and calcineurin after myocardial infarction in the noninfarcted area

The pJNK:JNK ratio decreased significantly in the hypertrophic, noninfarcted area of WT-MI mice when compared with sham-operated WT mice (−51%; $p < 0.05$) (Fig. 3). In contrast, the pJNK:JNK ratio in KO-MI mice was not significantly regulated when compared with KO mice but significantly up-regulated when compared with WT-MI mice (+78%; $p < 0.05$). Whereas the ratio between pJNK and

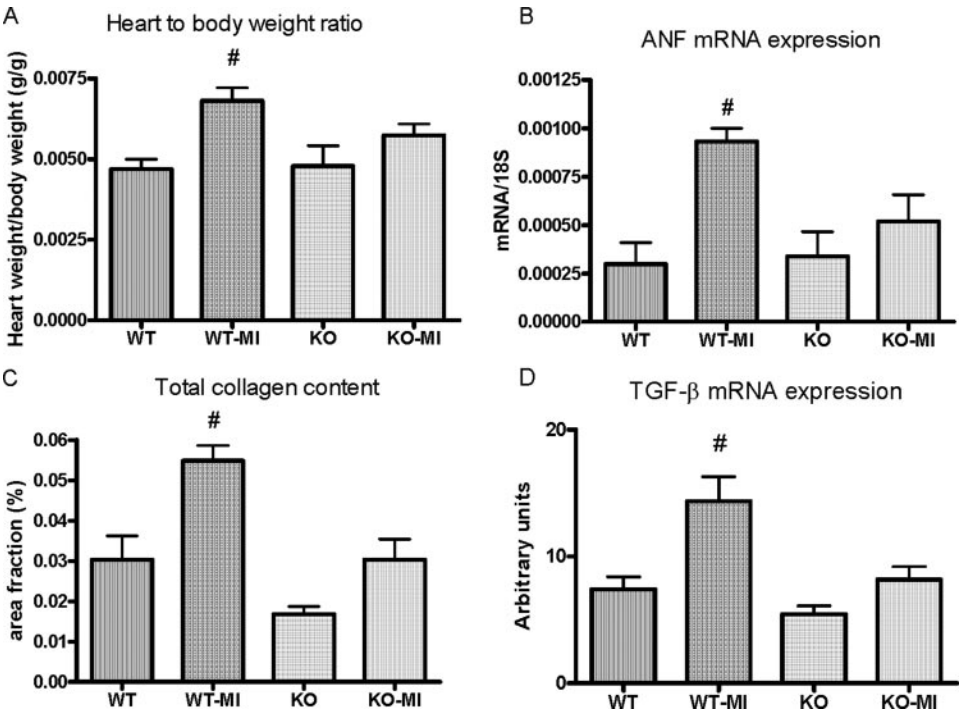

FIGURE 1. Left ventricular remodeling of the noninfarcted area. LV remodeling was indexed by the determination of heart-to-body-weight ratio (*A*), ANF mRNA expression (*B*), total collagen content (*C*), and TGF-β mRNA expression (*D*) (n = 6 per group). Data are expressed as mean ± SEM. #, $p < 0.05$ vs WT, KO, and KO-MI.

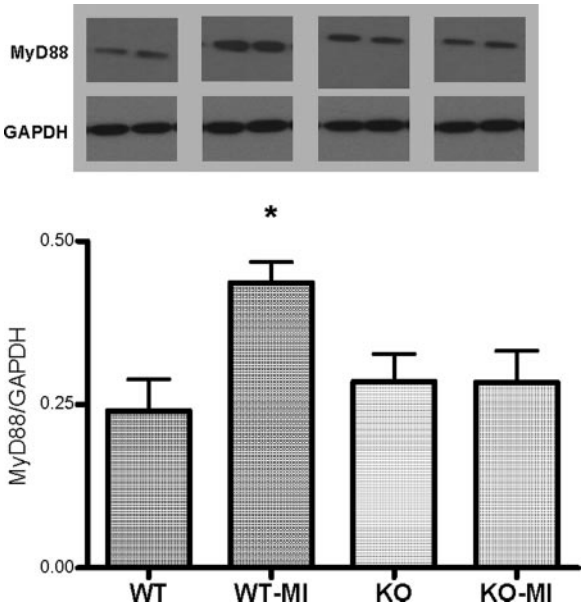

FIGURE 2. MyD88 expression in the noninfarcted area. Protein content of MyD88 in the noninfarcted area was determined using Western blot analyses ($n = 6$ per group). Representative blots of two animals per group were shown above the specific column. Data are expressed as mean ± SEM. *, $p < 0.05$ vs WT, KO, and KO-MI.

calcineurin was not significantly regulated in WT-MI mice when compared with WT mice, it was significantly up-regulated in KO-MI mice when compared with KO mice (9.3-fold; $p < 0.05$) (Fig. 3).

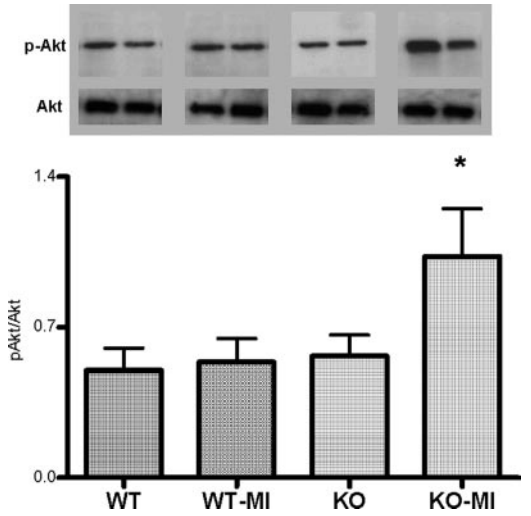

FIGURE 4. Activation of Akt in the noninfarcted area. The ratio of the protein content of pAkt:Akt in the noninfarcted area was determined using Western blot analyses ($n = 6$ per group). Representative blots of two animals per group were shown above the specific column. Data are expressed as mean ± SEM. *, $p < 0.05$ vs WT, WT-MI, and KO.

Protein activation of Akt after myocardial infarction in the noninfarcted area

The ratio of pAkt:Akt was not significantly regulated in WT mice when compared with WT-MI and KO mice. In contrast, this ratio

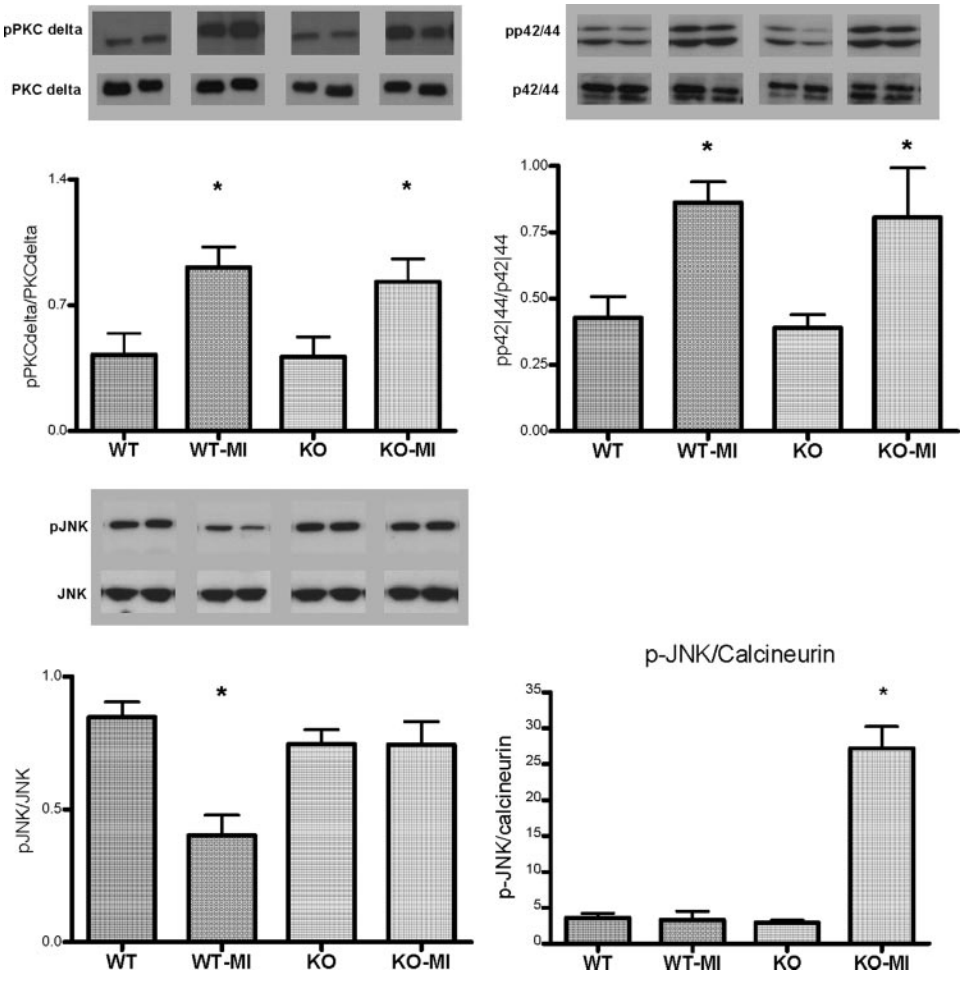

FIGURE 3. Activation of PKCδ, p42/44, JNK, and pJNK/calcineurin ratio after myocardial infarction in the noninfarcted area. The ratios of the protein content of pPKCδ:PKCδ, pp42.44:p42/44, pJNK:JNK, and pJNK:calcineurin in the noninfarcted area were determined using Western blot analyses ($n = 6$ per group). Representative blots of two animals per group were shown above the specific column. Data are expressed as mean ± SEM. *, $p < 0.05$ vs WT and KO.

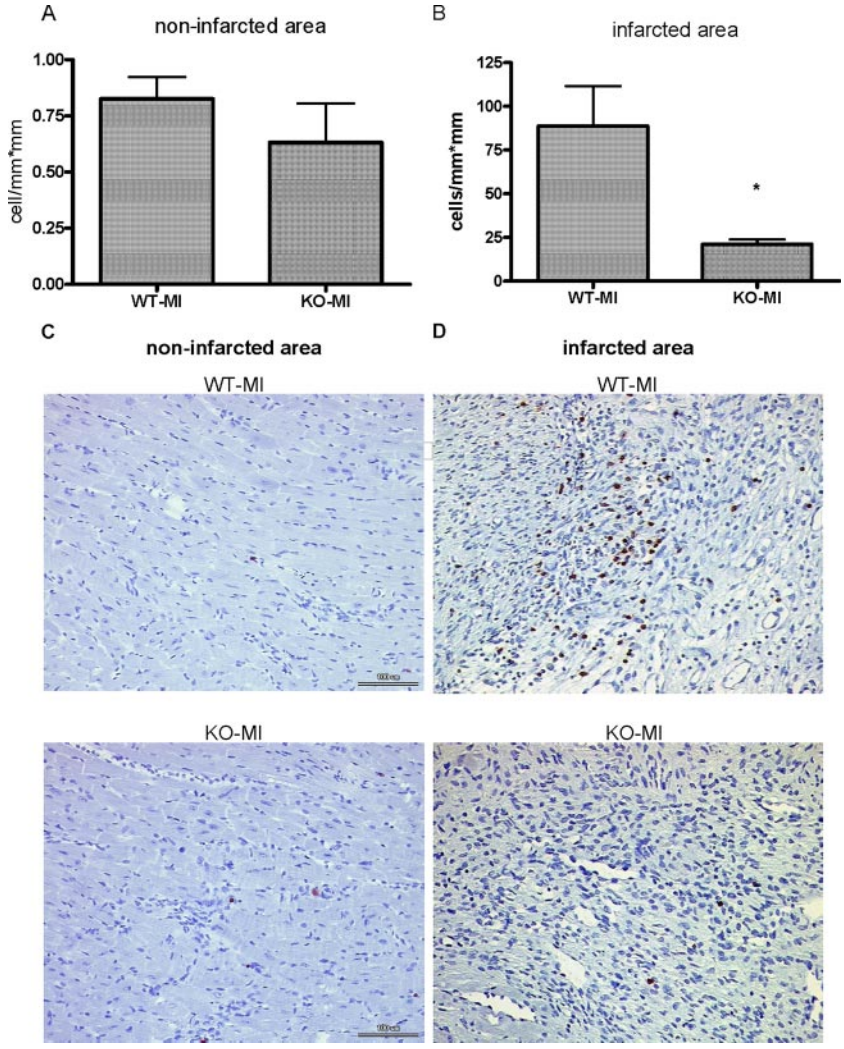

FIGURE 5. CD3-positive cells in the infarcted and noninfarcted areas. Infiltration of CD3-positive leukocytes (red) in the noninfarcted (*A*) and infarcted (*B*) areas were assessed by immunostaining and quantified by digital image analysis ($n = 6$ per group). Representative pictures are shown in *C* and *D*. Data are expressed as mean ± SEM. ∗, $p < 0.05$ vs WT-MI.

was significantly up-regulated in KO-MI mice when compared with KO mice (+79%; $p < 0.05$) and also when compared with WT-MI mice (+88%; $p < 0.05$) (Fig. 4).

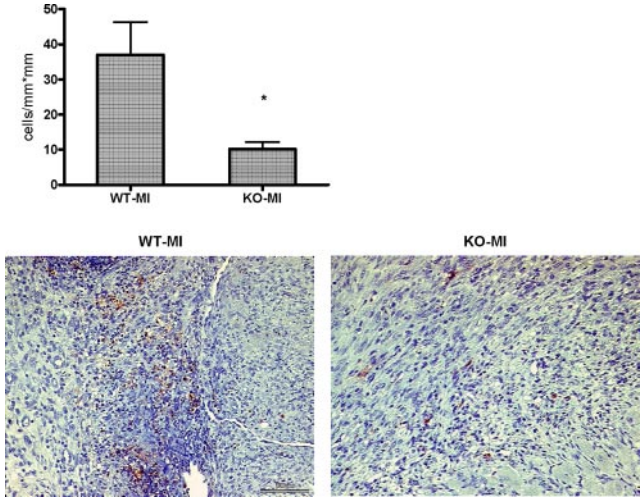

FIGURE 6. Apoptotic cells in the infarcted area. Apoptotic cells in the infarcted area was assessed by immunostaining of TUNEL-positive cells (red) and quantified by digital image analysis ($n = 6$ per group). Data are expressed as mean ± SEM. ∗, $p < 0.05$ vs WT-MI.

T-lymphocyte infiltration and apoptosis after myocardial infarction

Whereas CD3-positive cell infiltration into the noninfarcted area was similar in WT-MI and KO-MI mice (0.8 ± 0.2 vs 0.6 ± 0.3 cells/mm^2; NS), the infarcted area of WT-MI mice displayed markedly increased cell infiltration in comparison to the noninfarcted area (89 ± 23 vs 0.8 ± 0.2 cells/mm^2; $p < 0.05$). Furthermore, in the infarcted area of KO-MI mice cell infiltration was significantly decreased when compared with WT-MI mice (−76%; $p < 0.05$) (Fig. 5).

TUNEL staining indicated no increased content of apoptotic cells in the noninfarcted area of WT-MI mice when compared with sham-operated WT mice (0.004 ± 0.0002 vs 0.003 ± 0.0002 cells/mm^2). In contrast to this, the infarcted area of WT-MI mice displayed a significantly increased content of TUNEL-positive apoptotic cells when compared with WT mice. Also, reduced inflammatory response in the infarcted area of KO-MI mice was associated with a significantly reduced content of apoptotic cells in comparison with that of WT-MI mice (−73%; $p < 0.05$) (Fig. 6).

Mortality

KO-MI mice displayed improved survival of KO-MI when compared with WT-MI mice. As shown in Fig. 7, 28 days after the induction of MI, 62% of KO-MI mice but only 23% of WT-MI mice survived ($p < 0.0001$).

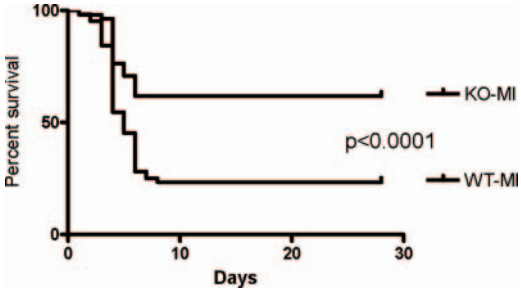

FIGURE 7. Survival rates after myocardial infarction. To determine survival after MI, WT-MI, and KO-MI mice were observed for 28 days ($n = 60$ per group).

Discussion

The salient finding of our study is that TLR4 deficiency reduces mortality in an animal model of MI mediated by an attenuation of LV remodeling. LV remodeling came to have an intense clinical application as a main mediator of morbidity and mortality after MI.

TLRs, known to mediate inflammatory response after viral, bacterial, or fungal infection, are also of special interest among different models of heart failure. Until today, current data suggested a role for TLR2 and TLR4 in the development of several types of heart failure, whereas other members of the TLR family do not appear to have been studied in regard to such conditions (8, 31). TLR4 has recently attracted considerable attention from studies in KO mice showing that this receptor is able to sufficiently trigger on pressure overload-induced concentric hypertrophy as well as on infarct size and survival due to ischemia/reperfusion injury (9, 16, 32–34). However, the ischemia/reperfusion model differs in comparison with the model of chronic ischemic cardiomyopathy induced after permanent occlusion of the left anterior descending artery. This model allows us to study the influence of TLR4 in postischemic remodeling and scar formation. In addition, the complex LV changes subsequent to MI, such as intense cytokine release or inflammatory cell migration into the infarcted area, are strongly associated with cardiac inflammation.

In this study we show that TLR4 modulates LV remodeling, independently of infarct size, in MI as a model of chronic ischemia as indexed by a reduction of LV hypertrophy, cardiac fibrosis, and TGF-β expression in KO-MI mice when compared with MI mice.

This receptor is at the same time of special interest for patients with coronary heart disease, because oxidized low density lipoprotein and heat shock proteins are parts of its endogenous ligands (10, 12, 35). Over and above this, clinical data showed a correlation between MI and the expression of TLR4-positive monocytes as well as a correlation between TLR4 Asp299Gly polymorphism and cardiovascular events (20, 36, 37).

We show here that TLR4 deficiency does not influence LV function under basal conditions. However, after induction of MI, reduced LV remodeling due to TLR4 deficiency did lead to a significant improvement of LV function along with reduced pulmonary edema and ANF expression, although infarct size was not found to differ between KO-MI and WT-MI mice.

We have shown previously that infiltrating immune cells are present in high concentrations in ischemic and nonischemic heart disease (24, 25, 38). In contrast, TLR4 is believed to activate these cells by its expression on the cell surface. We thus investigated further cell infiltration in scar formation and in noninfarcted LV tissue. We found in this case only a very little amount of CD3-positive cells in the noninfarcted area, suggesting that in this area it could be other cell types such as myocytes that are responsible for the beneficial effects of TLR4 deficiency after MI. In contrast, we found extensive infiltration of CD3-positive cells in scar formation of MI mice. This amount was significantly reduced in KO-MI mice, suggesting that TLR4-deficient, CD3-positive cells infiltrate to a lower degree into the heart after MI or, more likely, that this is a secondary effect due to less immune activation as a result of TLR4 deficiency.

Among other things, infiltration of immune cells, including CD3-positive lymphocytes, is also a matter that is capable of inducing apoptosis (4). In this study, we show that TLR4 leads to a reduction of this process without increasing the risk of ventricular rupture. Interestingly, changes in the numbers of infiltrating or apoptotic cells could not be found in the noninfarcted area, at least at the point in time investigated.

In summary, our data indicate that TLR4-controlled pathways can be activated through cardiac stress induced by chronic ischemia. After analyzing the changes in mortality, LV function, and cardiac remodeling, we conclude that TLR4 plays a pivotal role in MI.

To the best of our knowledge, no other data seem to exist about intracellular pathways that could indeed be responsible for these findings. The intracellular adapter protein MyD88 constitutes a key mediator for a variety of TLRs including TLR4 (39). Activation of the MyD88-dependent TLR pathway has been shown to play an emerging role in virus-mediated myocardial damage, pressure overload-induced LV hypertrophy, and ischemia/reperfusion injury (40–42). Because MI-induced MyD88 up-regulation was attenuated in KO mice when compared with KO-MI mice, we conclude that MyD88-dependent TLR4 signaling is associated with the initiation of postinfarction remodeling.

We were moreover interested in elucidating which additional downstream signals might possibly contribute to our findings. Among other factors, intracellular kinases such as PKCδ, p42/44, JNK, and calcineurin may contribute to TLR signaling (29). MyD88 may activate, via several signaling molecules, the TGF-β-activated kinase 1 (TAK1), which in turn activates among other things signaling pathways leading to the activation of p42/44 and JNK (43). PKCδ has been shown recently to bind to a TLR signaling complex, namely TIRAP/Mal, and thus participate in TLR signaling (44). In addition, Kang et al. showed a role of the phosphatase calcineurin in regulating TLR-activated pathways (30). Interestingly, all of these mediators are also believed to be key mediators in the development of LV remodeling (14). With this in mind, we investigated three kinases known to contribute to TLR4/MyD88 signaling that are also known to be involved in cardiac remodeling (45–47). In this respect, we determined p42/44, PKCδ, and JNK values. P42/44 and PKCδ were markedly activated in WT-MI mice to a similar degree as that seen in KO-MI, suggesting that both kinases are not controlled by TLR4, at least at the point in time investigated in our model. In contrast to p42/44 and PKCδ, another intracellular kinase, namely JNK, was affected by both MI and TLR4. Reduced activation of JNK is known to induce directly a severe LV hypertrophy (48). KO-MI mice displayed a significantly increased JNK expression when compared with WT-MI mice, suggesting that the JNK pathway may be involved in TLR4-triggered LV remodeling after MI. Anti-hypertrophic effects of JNK can also be mediated by cross-talk to calcineurin signaling as reported by Liang and Molkentin (48) Because it is known that JNK is primarily dedicated to inhibiting the calcineurin-induced dephosphorylation of the cytosolic fraction of the transcription factor of activated T cells (NFAT), it can in turn prevent any activation of NFAT by migration toward the nucleus. Therefore, we also studied calcineurin expression and determined a pJNK/calcineurin ratio in our model. Whereas the ratio was similar in WT, WT-MI, and KO mice, we found a marked increase in this ratio in KO-MI

mice, suggesting that TLR4 mediates alterations in the JNK/calcineurin ratio, thus contributing to LV hypertrophy as seen in the WT-MI mice of our study. In addition, we investigated the serine-threonine kinase Akt, which, among other things, is implicated in cell survival (49).

Akt has been shown to be up-regulated in models of preconditioning, thereby exerting cardioprotective effects, which include cell survival, contributing to a limitation of infarct size (49, 50). However, in chronic cardiac ischemia it is known that Akt is not regulated, and this has also been shown in our study (51). We found it to be of interest as well that TLR4 deficiency was associated with an activation of cardiac Akt. Thus, it is intriguing to speculate that Akt activation is suppressed by TLR4-controlled mechanisms in the chronic ischemic heart and that Akt up-regulation might in fact contribute to the cardioprotective effects seen in TLR4-deficient mice with chronic ischemic heart disease.

In summary, TLR4 deficiency was found to lead to improved survival and LV function mediated by attenuation of LV remodeling in a mouse model of MI. Our data show that a dysregulation of JNK and Akt and the imbalance between JNK and calcineurin, but not p42/44 and PKCδ, are associated with TLR4-mediated postinfarction remodeling. Therefore, it may be possible that TLR4 could be a promising therapeutic target for the treatment of ischemic heart disease. However, further studies will have to prove this hypothesis. They will have to show whether or not any specific TLR4 antagonists already available may indeed be sufficient in protecting the heart against LV remodeling after M, and whether or not this strategy in the future might even be capable of augmenting the current standard therapy.

Acknowledgments

We thank Kerstin Puhl for excellent technical assistance. The TLR4$^{-/-}$ mice were provided by Marina Freudenberg (Max-Planck-Institute for Immunobiology, Freiburg, Germany).

Disclosures

The authors have no financial conflict of interest.

References

1. Lewis, E. F., L. A. Moye, J. L. Rouleau, F. M. Sacks, J. M. Arnold, J. W. Warnica, G. C. Flaker, E. Braunwald, and M. A. Pfeffer. 2003. Predictors of late development of heart failure in stable survivors of myocardial infarction: the CARE study. *J. Am. Coll. Cardiol.* 42: 1446–1453.
2. Opie, L. H., P. J. Commerford, B. J. Gersh, and M. A. Pfeffer. 2006. Controversies in ventricular remodelling. *Lancet* 367: 356–367.
3. Liao, Y. H., and X. Cheng. 2006. Autoimmunity in myocardial infarction. *Int. J. Cardiol.* 112: 21–26.
4. Frangogiannis, N. G. 2006. Targeting the inflammatory response in healing myocardial infarcts. *Curr. Med. Chem.* 13: 1877–1893.
5. Fan, J., Y. Li, R. M. Levy, J. J. Fan, D. J. Hackam, Y. Vodovotz, H. Yang, K. J. Tracey, T. R. Billiar, and M. A. Wilson. 2007. Hemorrhagic shock induces NAD(P)H oxidase activation in neutrophils: role of HMGB1-TLR4 signaling. *J. Immunol.* 178: 6573–6580.
6. Frisancho-Kiss, S., S. E. Davis, J. F. Nyland, J. A. Frisancho, D. Cihakova, M. A. Barrett, N. R. Rose, and D. Fairweather. 2007. Cutting edge: cross-regulation by TLR4 and T cell Ig mucin-3 determines sex differences in inflammatory heart disease. *J. Immunol.* 178: 6710–6714.
7. Nozaki, N., T. Shishido, Y. Takeishi, and I. Kubota. 2004. Modulation of doxorubicin-induced cardiac dysfunction in toll-like receptor-2-knockout mice. *Circulation* 110: 2869–2874.
8. Shishido, T., N. Nozaki, S. Yamaguchi, Y. Shibata, J. Nitobe, T. Miyamoto, H. Takahashi, T. Arimoto, K. Maeda, M. Yamakawa, et al. 2003. Toll-like receptor-2 modulates ventricular remodeling after myocardial infarction. *Circulation* 108: 2905–2910.
9. Oyama, J., C. Blais, Jr., X. Liu, M. Pu, L. Kobzik, R. A. Kelly, and T. Bourcier. 2004. Reduced myocardial ischemia-reperfusion injury in toll-like receptor 4-deficient mice. *Circulation* 109: 784–789.
10. Smiley, S. T., J. A. King, and W. W. Hancock. 2001. Fibrinogen stimulates macrophage chemokine secretion through toll-like receptor 4. *J. Immunol.* 167: 2887–2894.
11. Jones, P. H., M. H. Davidson, E. A. Stein, H. E. Bays, J. M. McKenney, E. Miller, V. A. Cain, and J. W. Blasetto. 2003. Comparison of the efficacy and safety of rosuvastatin versus atorvastatin, simvastatin, and pravastatin across doses (STELLAR* Trial). *Am. J. Cardiol.* 92: 152–160.
12. Ohashi, K., V. Burkart, S. Flohe, and H. Kolb. 2000. Cutting edge: heat shock protein 60 is a putative endogenous ligand of the toll-like receptor-4 complex. *J. Immunol.* 164: 558–561.
13. Akira, S., and K. Takeda. 2004. Toll-like receptor signalling. *Nat. Rev. Immunol.* 4: 499–511.
14. Heineke, J., and J. D. Molkentin. 2006. Regulation of cardiac hypertrophy by intracellular signalling pathways. *Nat. Rev. Mol. Cell Biol.* 7: 589–600.
15. Boyd, J. H., S. Mathur, Y. Wang, R. M. Bateman, and K. R. Walley. 2006. Toll-like receptor stimulation in cardiomyoctes decreases contractility and initiates an NF-κB dependent inflammatory response. *Cardiovasc. Res.* 72: 384–393.
16. Shimamoto, A., A. J. Chong, M. Yada, S. Shomura, H. Takayama, A. J. Fleisig, M. L. Agnew, C. R. Hampton, C. L. Rothnie, D. J. Spring, et al. 2006. Inhibition of Toll-like receptor 4 with eritoran attenuates myocardial ischemia-reperfusion injury. *Circulation* 114 (Suppl. 1): I270–I274.
17. Ha, T., Y. Li, F. Hua, J. Ma, X. Gao, J. Kelley, A. Zhao, G. E. Haddad, D. L. Williams, I. W. Browder, et al. 2005. Reduced cardiac hypertrophy in toll-like receptor 4-deficient mice following pressure overload. *Cardiovasc. Res.* 68: 224–234.
18. Baumgarten, G., P. Knuefermann, G. Schuhmacher, V. Vervolgyi, J. von Rappard, U. Dreiner, K. Fink, C. Djoufack, A. Hoeft, C. Grohe, et al. 2006. Toll-like receptor 4, nitric oxide, and myocardial depression in endotoxemia. *Shock* 25: 43–49.
19. Satoh, M., Y. Shimoda, C. Maesawa, T. Akatsu, Y. Ishikawa, Y. Minami, K. Hiramori, and M. Nakamura. 2006. Activated toll-like receptor 4 in monocytes is associated with heart failure after acute myocardial infarction. *Int. J. Cardiol.* 109: 226–234.
20. Methe, H., J. O. Kim, S. Kofler, M. Weis, M. Nabauer, and J. Koglin. 2005. Expansion of circulating Toll-like receptor 4-positive monocytes in patients with acute coronary syndrome. *Circulation* 111: 2654–2661.
21. Poltorak, A., X. He, I. Smirnova, M. Y. Liu, C. Van Huffel, X. Du, D. Birdwell, E. Alejos, M. Silva, C. Galanos, et al. 1998. Defective LPS signaling in C3H/HeJ and C57BL/10ScCr mice: mutations in Tlr4 gene. *Science* 282: 2085–2088.
22. Tschope, C., D. Westermann, N. Dhayat, S. Dhayat, C. Altmann, P. Steendijk, H. P. Schultheiss, and T. Walther. 2005. Angiotensin AT2 receptor deficiency after myocardial infarction: its effects on cardiac function and fibrosis depend on the stimulus. *Cell Biochem. Biophys.* 43: 45–52.
23. Bien, S., A. Riad, C. A. Ritter, M. Gratz, F. Olshausen, D. Westermann, M. Grube, T. Krieg, S. Ciecholewski, S. B. Felix, et al. 2007. The endothelin receptor blocker bosentan inhibits doxorubicin-induced cardiomyopathy. *Cancer Res.* 67: 10428–10435.
24. Westermann, D., S. Rutschow, S. Jager, A. Linderer, S. Anker, A. Riad, T. Unger, H. P. Schultheiss, M. Pauschinger, and C. Tschöpe. 2007. Contributions of inflammation and cardiac matrix metalloproteinase activity to cardiac failure in diabetic cardiomyopathy: the role of angiotensin type 1 receptor antagonism. *Diabetes* 56: 641–646.
25. Riad, A., D. Unger, J. Du, D. Westermann, Z. Mohr, M. Sobirey, M. Dorenkamp, H. P. Schultheiss, and C. Tschope. 2007. Chronic inhibition of p38MAPK improves cardiac and endothelial function in experimental diabetes mellitus. *Eur. J. Pharmacol.* 554: 40–45.
26. Tschope, C., T. Walther, J. Koniger, F. Spillmann, D. Westermann, F. Escher, M. Pauschinger, J. B. Pesquero, M. Bader, H. P. Schultheiss, and M. Noutsias. 2004. Prevention of cardiac fibrosis and left ventricular dysfunction in diabetic cardiomyopathy in rats by transgenic expression of the human tissue kallikrein gene. *FASEB J.* 18: 828–835.
27. Li, J., S. Leschka, S. Rutschow, P. L. Schwimmbeck, L. Husmann, M. Noutsias, D. Westermann, W. Poller, H. Zeichhardt, K. Klingel, et al. 2007. Immunomodulation by interleukin-4 suppresses matrix metalloproteinases and improves cardiac function in murine myocarditis. *Eur. J. Pharmacol.* 554: 60–68.
28. Livak, K. J., and T. D. Schmittgen. 2001. Analysis of relative gene expression data using real-time quantitative PCR and the $2(-\Delta\Delta C_T)$ method. *Methods* 25: 402–408.
29. O'Neill, L. A., and A. G. Bowie. 2007. The family of five: TIR-domain-containing adaptors in Toll-like receptor signalling. *Nat. Rev. Immunol.* 7: 353–364.
30. Kang, Y. J., B. Kusler, M. Otsuka, M. Hughes, N. Suzuki, S. Suzuki, W. C. Yeh, S. Akira, J. Han, and P. P. Jones. 2007. Calcineurin negatively regulates TLR-mediated activation pathways. *J. Immunol.* 179: 4598–4607.
31. Sakata, Y., J. W. Dong, J. G. Vallejo, C. H. Huang, J. S. Baker, K. J. Tracey, O. Tacheuchi, S. Akira, and D. L. Mann. 2007. Toll-like receptor 2 modulates left ventricular function following ischemia-reperfusion injury. *Am. J. Physiol.* 292: H503–H509.
32. Hua, F., T. Ha, J. Ma, Y. Li, J. Kelley, X. Gao, I. W. Browder, R. L. Kao, D. L. Williams, and C. Li. 2007. Protection against myocardial ischemia/reperfusion injury in TLR4-deficient mice is mediated through a phosphoinositide 3-kinase-dependent mechanism. *J. Immunol.* 178: 7317–7324.
33. Kim, S. C., A. Ghanem, H. Stapel, K. Tiemann, P. Knuefermann, A. Hoeft, R. Meyer, C. Grohe, A. A. Knowlton, and G. Baumgarten. 2007. Toll-like receptor 4 deficiency: smaller infarcts, but no gain in function. *BMC Physiol.* 7: 5.
34. Stapel, H., S. C. Kim, S. Osterkamp, P. Knuefermann, A. Hoeft, R. Meyer, C. Grohe, and G. Baumgarten. 2006. Toll-like receptor 4 modulates myocardial ischaemia-reperfusion injury: role of matrix metalloproteinases. *Eur. J. Heart Fail.* 8: 665–672.
35. Jones, P. H., J. M. McKenney, D. G. Karalis, and J. Downey. 2005. Comparison of the efficacy and safety of atorvastatin initiated at different starting doses in patients with dyslipidemia. *Am. Heart J.* 149: e1.
36. Boekholdt, S. M., W. R. Agema, R. J. Peters, A. H. Zwinderman, E. E. van der Wall, P. H. Reitsma, J.J. Kastelein, and J. W. Jukema. 2003.

Variants of Toll-like receptor 4 modify the efficacy of statin therapy and the risk of cardiovascular events. *Circulation* 107: 2416–2421.
37. Ameziane, N., T. Beillat, P. Verpillat, S. Chollet-Martin, M. C. Aumont, P. Seknadji, M. Lamotte, D. Lebret, V. Ollivier, and D. de Prost. 2003. Association of the Toll-like receptor 4 gene Asp299Gly polymorphism with acute coronary events. *Arterioscler. Thromb. Vasc. Biol.* 23: e61–e64.
38. Tschope, C., F. Spillmann, C. Altmann, M. Koch, D. Westermann, N. Dhayat, S. Dhayat, J. L. Bascands, L. Gera, S. Hoffman, et al. 2004. The bradykinin B1 receptor contributes to the cardioprotective effects of AT1 blockade after experimental myocardial infarction. *Cardiovasc Res.* 61: 559–569.
39. Kawai, T., and S. Akira. 2005. Toll-like receptor downstream signaling. *Arthritis Res. Ther.* 7: 12–19.
40. Ha, T., F. Hua, Y. Li, J. Ma, X. Gao, J. Kelley, A. Zhao, G. E. Haddad, D. L. Williams, I. W. Browder, et al. 2006. Blockade of MyD88 attenuates cardiac hypertrophy and decreases cardiac myocyte apoptosis in pressure overload-induced cardiac hypertrophy in vivo. *Am. J. Physiol.* 290: H985–H994.
41. Fuse, K., G. Chan, Y. Liu, P. Gudgeon, M. Husain, M. Chen, W. C. Yeh, S. Akira, and P. P. Liu. 2005. Myeloid differentiation factor-88 plays a crucial role in the pathogenesis of coxsackievirus B3-induced myocarditis and influences type I interferon production. *Circulation* 112: 2276–2285.
42. Hua, F., T. Ha, J. Ma, X. Gao, J. Kelley, D. L. Williams, I. W. Browder, R. L. Kao, and C. Li. 2005. Blocking the MyD88-dependent pathway protects the myocardium from ischemia/reperfusion injury in rat hearts. *Biochem. Biophys. Res. Commun.* 338: 1118–1125.
43. Dong, C., R. J. Davis, and R. A. Flavell. 2002. MAP kinases in the immune response. *Annu. Rev. Immunol.* 20: 55–72.
44. Kubo-Murai, M., K. Hazeki, N. Sukenobu, K. Yoshikawa, K. Nigorikawa, K. Inoue, T. Yamamoto, M. Matsumoto, T. Seya, N. Inoue, and O. Hazeki. 2007. Protein kinase Cδ binds TIRAP/Mal to participate in TLR signaling. 2007. *Mol. Immunol.* 44: 2257–2264.
45. Biesalski, H. K., B. Bueno de Mesquita, A. Chesson, F. Chytil, R. Grimble, R. J. Hermus, J. Kohrle, R. Lotan, K. Norpoth, U. Pastorino, and D. Thurnham. 1998. European consensus statement on lung cancer: risk factors and prevention: lung cancer panel. 1998. *CA Cancer J. Clin.* 48: 167–176.
46. Chen, L., H. Hahn, G. Wu, C. H. Chen, T. Liron, D. Schechtman, G. Cavallaro, L. Banci, Y. Guo, R. Bolli, et al. 2001. Opposing cardioprotective actions and parallel hypertrophic effects of δ PKC and ε PKC. 2001. *Proc. Natl. Acad. Sci. USA* 98: 11114–11119.
47. Azuma, H., M. Sugimoto-Tokushima, K. Tanaka, Y. Ikenoue, S. Ito, and M. Ishikawa. 1989. α 1-adrenoceptor antagonist activity of novel pyrimidine derivatives (SHI437 and IK29) in rabbit aorta and trigone of the bladder. *Br. J. Pharmacol.* 96: 1000–1006.
48. Liang, Q., and J. D. Molkentin. 2003. Redefining the roles of p38 and JNK signaling in cardiac hypertrophy: dichotomy between cultured myocytes and animal models. *J. Mol. Cell. Cardiol.* 35: 1385–1394.
49. Cantley, L. C. 2002. The phosphoinositide 3-kinase pathway. *Science* 296: 1655–1657.
50. Hausenloy, D. J., and D. M. Yellon. 2006. Survival kinases in ischemic preconditioning and postconditioning. *Cardiovasc. Res.* 70: 240–253.
51. Ravingerova, T., J. Matejikova, J. Neckar, E. Andelova, and F. Kolar. 2007. Differential role of PI3K/Akt pathway in the infarct size limitation and antiarrhythmic protection in the rat heart. *Mol. Cell. Biochem.* 297: 111–120.